Supporting Information:

Expanding the Horizons of Thermodynamic Landscape and Optoelectronic Properties of Soft 2D Hybrid Perovskites MHy_2PbX_4

Szymon Sobczak*[,a], Andrzej Nowok[b,c], Jan K. Zaręba[d], Aleksandra Półrolniczak,[a] Kinga Roszak,[a] Anna Z. Szeremeta[e], Błażej Dziuk[d], Filip Dybała[f], Sebastian Pawlus[e], Robert Kudrawiec[f], Adam Sieradzki[c], Mirosław Mączka[g],* Andrzej Katrusiak *[,a]

[a] *Faculty of Chemistry, Adam Mickiewicz University, Uniwersytetu Poznanskiego 8, 61-614 Poznan, Poland*
[b] *Laboratoire National des Champs Magnétiques Intenses, EMFL, CNRS UPR 3228, Université Toulouse, Université Toulouse 3, INSA-T, Toulouse 31400, France*
[c] *Department of Experimental Physics, Wrocław University of Science and Technology, Wybrzeże Wyspiańskiego 27, 50-370, Wrocław, Poland*
[d] *Institute of Advanced Materials, Wrocław University of Science and Technology, Wybrzeże Wyspiańskiego 27, 50-370, Wrocław, Poland*
[e] *August Chełkowski Institute of Physics, University of Silesia in Katowice, ul. 75 Pułku Piechoty 1, 41-500 Chorzów, Poland*
[f] *Department of Semiconductor Materials Engineering, Wrocław University of Science and Technology, Wybrzeże Wyspiańskiego 27, 50-370, Wrocław, Poland*
[g] *Institute of Low Temperature and Structure Research, Polish Academy of Sciences, Okólna 2, 50-422 Wrocław, Poland*

Reassingment of phase II-MHy_2PbI_4

The X-ray diffraction experiments performed at elevated temperatures, from 300 to 370 K, revealed unassingned layer of reflections appearing perpendicular to direction [001] below 320 K (Figure S1). The low intensity of the reflections is connected with the strong absorbtion of the X-ray radiation by the crystalline sample and the character of temperature-induced phase transition.

(a) 300 K (b) 310 K

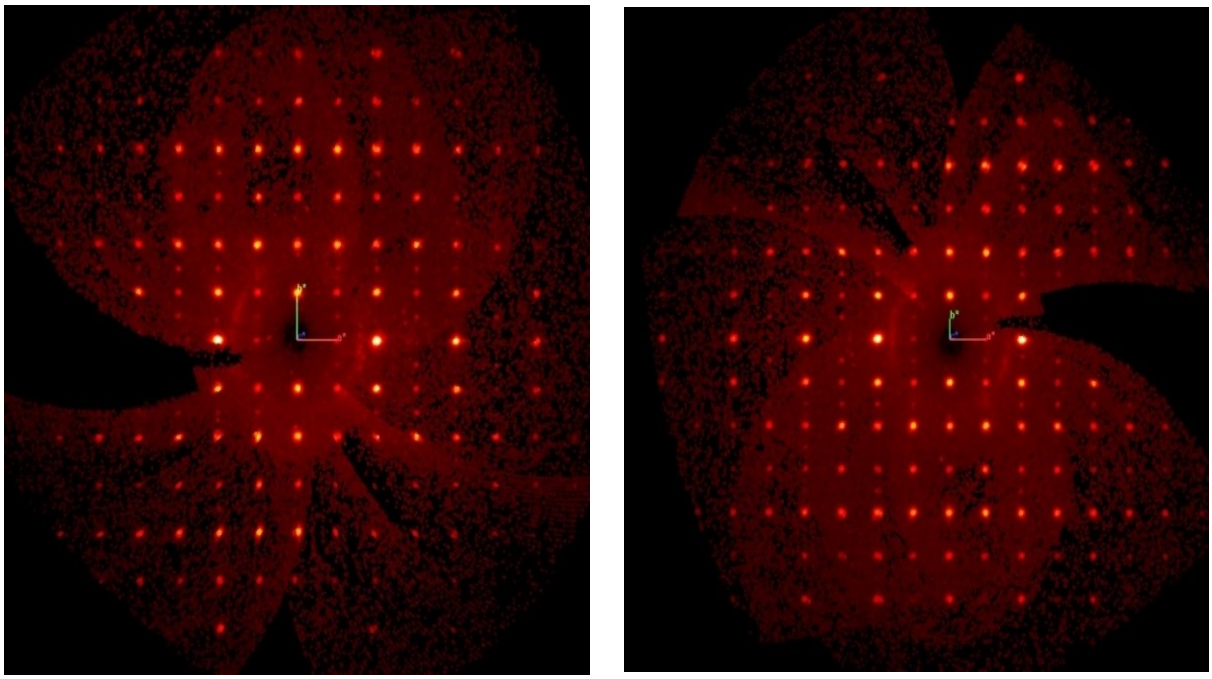

Figure S1. The reconstruction of hk*0* layers of II-MHy_2PbI_4 collected at (a) 300 K and (b) 310 K in respect to phases reported in ref 24. A row of unassigned reflections were indicated for each image.

Ferroelectricity of phase IV-MHy_2PbI_4

In order to understand the ferroelectric properties of VI-MHy_2PbI_4, we closely examine the ferroelectric phase III of MHy_2PbBr_4, which provides a structural and functional prototype. The study described by Mączka et al. (*Chem. Mater*. 2021, 33, 7, 2331–2342) reveals that a strong

dielectric response and spontaneous polarization in phase III of MHy_2PbBr_4 originates in the orientation of the MHy^+ cations and the distortion of the polyanionic framework.

Although the both phases share isomorphic features and comparable octahedral distortions, the specific reorientation of cations in VI-MHy_2PbI_4 suggests a unique redistribution of dipole moments, which is expected to be the primary contributor to its ferroelectric properties. Furthermore, the slight shifts in halogen positions in VI-MHy_2PbI_4, could modulate the polarization field, reinforcing the effect induced by cation rotation. Consequently, the ferroelectric character of VI-MHy_2PbI_4 obtained at high-pressure emerges from a multifaceted interaction of these structural charecteristics, mirroring the ferroelectric determinants of III-

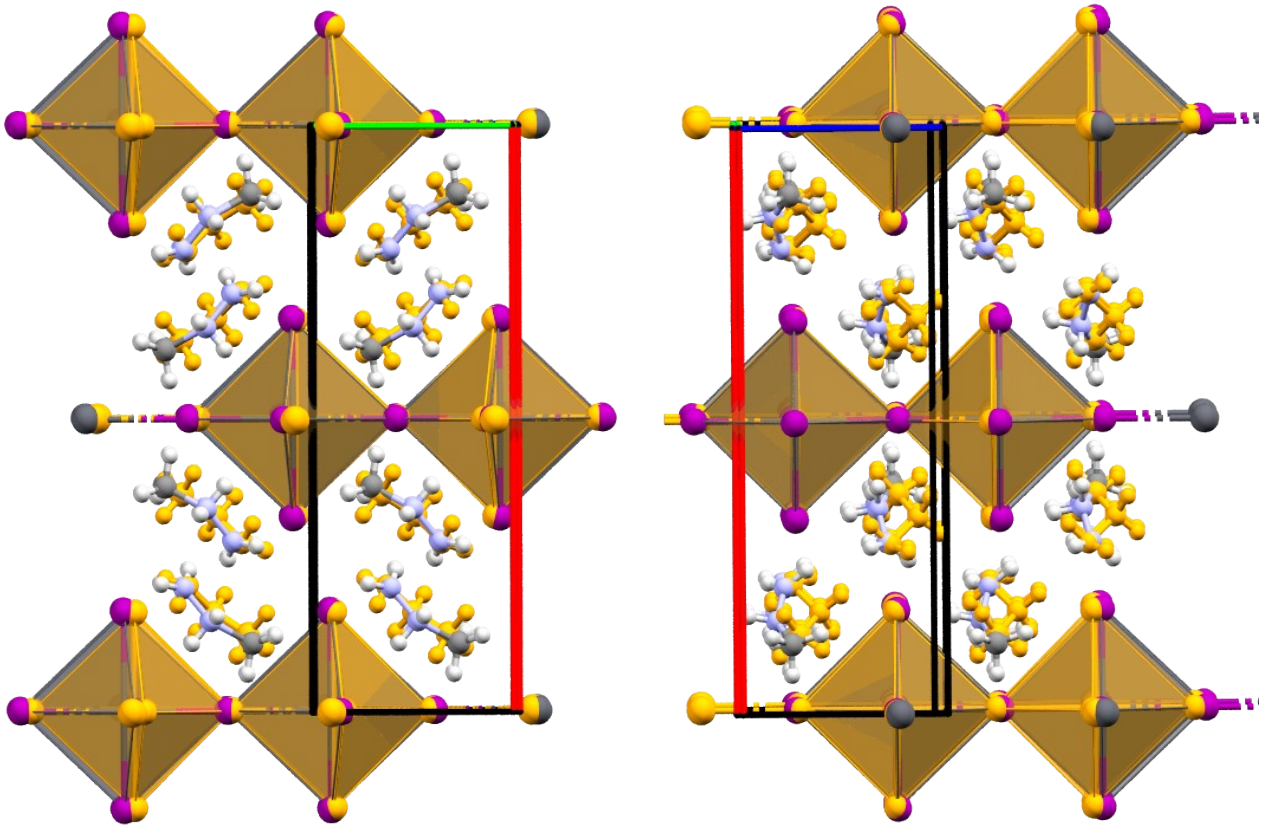

MHy_2PbBr_4, yet exhibiting inherent distinctions owing to the halogen variation.

Figure S4. The unit-cell of of VI-MHy_2PbI_4 at 1.15 GPa with atom-specific color coding: lead (black), iodine (purple), carbon (grey), nitrogen (blue), and hydrogen (white) superimposed on structure of ambient-pressure III-MHy_2PbBr_4 (coloured yellow) with respect to the coordination sphere of the Pb^{2+} metal center.

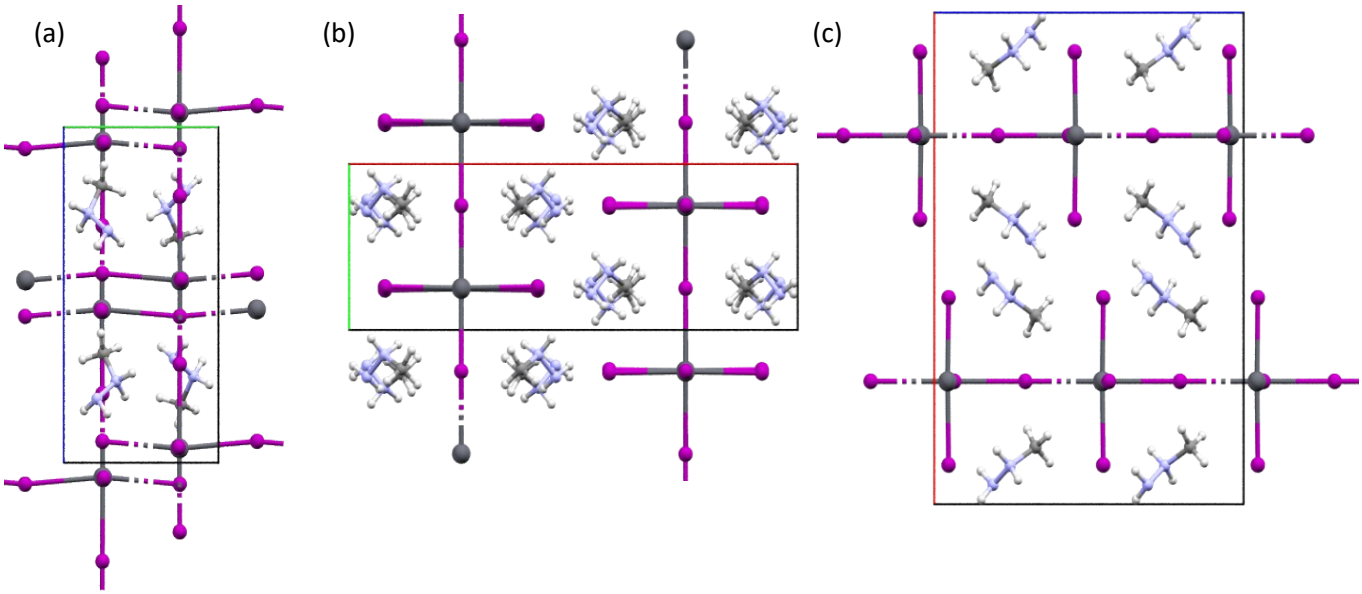

Figure S2. The unit-cell projection of II-MHy_2PbI_4 projected along (a) [100]; (b) [010] and (c) [001] at 300K.

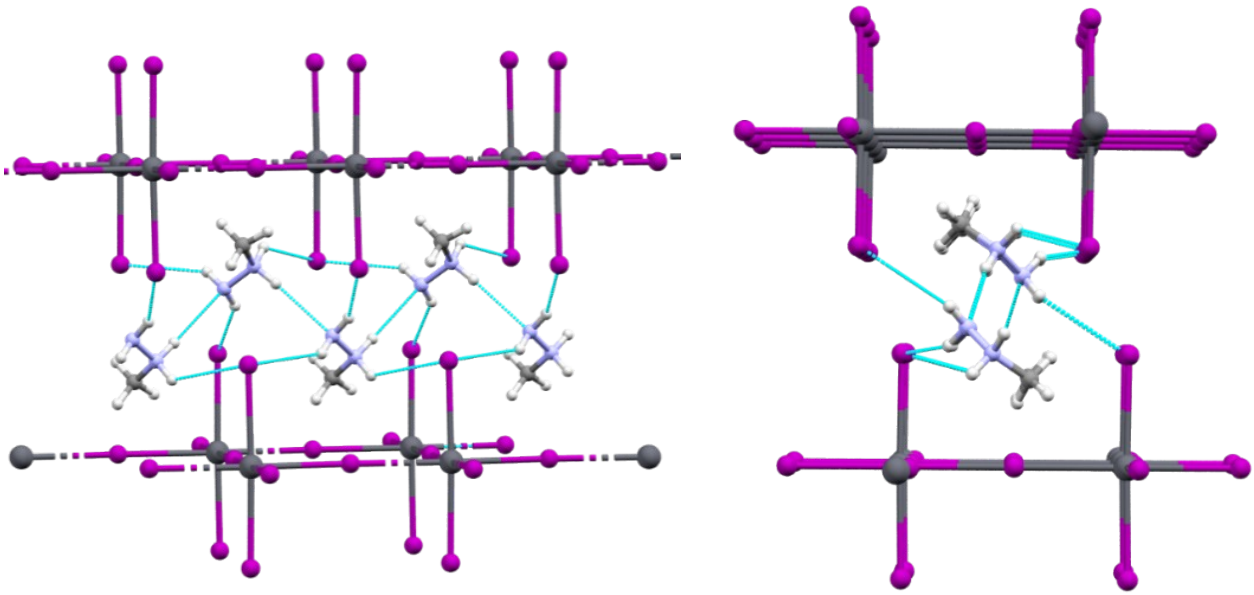

Figure S3. The H-bond pattern present in II-MHy_2PbI_4 at 300 K.

Table S1. The Pb–I bond length in phase **V** at different pressures.

Bonds (Å)	0.22 GPa	1.00 GPa
Pb1-I1	3.18900	3.17200
Pb1-I1^{i}	3.18900	3.17200
Pb1-I2	3.11300	3.09100
Pb1-I2^{ii}	3.11300	3.09100
Pb1-I3	3.18000	3.16000
Pb1-I3^{iii}	3.18000	3.16000
d (Å)	3.16067	3.14100
Δ*d*	0.00115	0.00127

i = x, y, 1 + z; ii = -x, y, z; iii = x, 1 + y, z

Table S2. The distortions of the individual PbI_6 octahedra in phase **VI** at different pressures.

Bonds (Å)	1.30 GPa	1.70 GPa	2.10 GPa	2.64 GPa	3.00 GPa
Pb1-I1	3.14300	3.14200	3.16200	3.17700	3.12500
Pb1-I1^{i}	3.14300	3.14200	3.16200	3.17700	3.12500
Pb1-I2	3.00900	3.09100	3.09600	3.02600	3.01900
Pb1-I2^{ii}	3.00900	3.09100	3.09600	3.02600	3.01900
Pb1-I3	3.15400	3.15700	3.11800	3.10600	3.13900
Pb1-I3^{iii}	3.15400	3.15700	3.11800	3.10600	3.13900
d (Å)	3.10200	3.13000	3.12533	3.10300	3.09433
Δd	0.00434	0.00080	0.00075	0.00380	0.00287

Bonds (Å)	3.30 GPa	3.74 GPa	4.20 GPa		3.30 GPa	3.74 GPa	4.20 GPa
Pb1A-I1A	3.09000	3.04100	3.09900	Pb1b-I1b	3.10000	3.10800	3.11200
Pb1A-I1A'	3.11900	3.13500	3.12600	Pb1b-I1b'	3.10800	3.12100	3.12300
Pb1A-I2A	2.98600	3.18100	2.96700	Pb1b-I2b	2.99200	3.29900	3.09300

Pb1A-I3A	3.05400	3.03500	3.05900	Pb1b-I3b	3.05400	3.06300	3.05400
Pb1A-I3A"	3.14600	3.13500	3.18400	Pb1b-I3b"	3.16700	3.18200	3.20500
Pb1A-I4A	2.98300	3.02600	3.12100	Pb1b-I4b	2.97500	2.89500	2.97200
d	3.06300	3.09217	3.09267	*d*	3.06600	3.11133	3.09317
Δ*d*	0.00386	0.00364	0.00454	Δ*d*	0.00450	0.01491	0.00499

i =1 - *x*, -½+ *y*, 1- *z*; *ii* = -1 + *x*, *y*, *z*

Table S3. The bond length in phase **VII** at different pressures.

Table S4. Bond angle variance of the individual PbI_6 octahedra in phase **V** at different pressures.

Bond Angles (°)	0.22 GPa	1.00 GPa
I1-Pb1- I2	89.98	90.03
I1-Pb1- I 2^{i}	89.98	90.03
I1-Pb1-I3	90.24	96.80
I1-Pb1-I3^{ii}	89.76	83.20
I3-Pb1-I1^{iii}	89.98	90.03
I3-Pb1-I2	89.98	90.03
I3-Pb1-I2^{i}	90.24	96.80
I2-Pb1-I1^{iii}	89.76	83.20
I2-Pb1-I3^{ii}	90.24	90.24
I1^{iii}-Pb1-I2^{i}	89.76	89.76
I2^{i}-Pb1-I3^{ii}	90.24	90.24
I1^{iii}-Pb1-I3^{ii}	89.76	89.76
σ(°)	0.04204	16.83582

i= -*x*,*y*,*z*; *ii*= *x*,1+*y*,*z*; *iii*= *x*,*y*,1+*z*

Table S5. Bond angle variance of the individual PbI_6 octahedra in phase **VI** at different pressures

Bond Angles (°)	1.30 GPa	1.70 GPa	2.10 GPa	2.64 GPa	3.00 GPa
I1-Pb1- I2	90.45	90.94	90.95	91.28	91.30
I1-Pb1- I 2^{i}	89.52	89.19	89.17	88.84	88.79
I1-Pb1-I3	96.73	101.13	101.24	101.98	102.55
I1-Pb1-I3^{ii}	85.76	84.40	84.44	84.14	83.75
I3-Pb1-I1^{iii}	90.45	90.94	90.95	91.28	91.30
I3-Pb1-I2	89.52	89.19	89.17	88.84	88.79
I3-Pb1-I2^{i}	94.30	95.60	95.55	95.95	96.29
I2-Pb1-I1^{iii}	83.21	78.86	78.77	77.93	77.40
I2-Pb1-I3^{ii}	90.17	90.38	90.37	90.33	90.20
I1^{iii}-Pb1-I2^{i}	89.81	89.53	89.54	89.54	89.66
I2^{i}-Pb1-I3^{ii}	90.17	90.38	90.37	90.33	90.20
I1^{iii}-Pb1-I3^{ii}	89.81	89.53	89.54	89.54	89.66

σ(°)	11.71458	28.59150	28.91331	33.23240	36.50077

i= 1/2-x,1.5-y,z; ii= x,y,-1+z; iii= x,1+y,z

Table S6. Bond angle variance of the individual PbI_6 octahedra in phase **VII** at different pressures.

Bond Angles (°)	3.30 GPa	3.74 GPa	4.20 GPa		3.30 GPa	3.74 GPa	4.20 GPa
I1A-Pb1A-I2A	88.84	87.82	95.10	I1B-Pb1B-I2B	92.82	94.72	87.17
I1A-Pb1A-I3A	79.61	78.56	93.94	I1B-Pb1B-I3B	102.64	105.57	108.61
I1A-Pb1A-I3A^{ii}	83.53	83.89	82.89	I1B-Pb1B-I3B^{ii}	97.21	97.28	88.20
I1A-Pb1A-I4A	92.95	91.45	88.12	I1B-Pb1B-I4B	90.86	88.64	91.04
I3A-Pb1A-I1A^{i}	101.27	104.69	107.26	I3B-Pb1B-I1B^{i}	77.52	75.14	94.43
I3A-Pb1A-I2A	86.14	91.58	85.15	I3B-Pb1B-I2B	95.96	100.58	84.20
I3A-Pb1A-I4A	98.73	93.69	85.58	I3B-Pb1B-I4B	87.21	84.20	87.41
I2A-Pb1A-I1A^{i}	86.05	91.34	87.78	I2B-Pb1B-I1B^{i}	86.53	84.55	88.54
I2A-Pb1A-I3A^{ii}	86.36	87.25	88.08	I2B-Pb1B-I3B^{ii}	87.99	86.99	99.32
I1Ai-Pb1A-I4A	92.04	89.08	88.51	I1B^{i}-Pb1B-I4B	89.78	92.04	92.61
I4A-Pb1A-I3A^{ii}	89.25	87.18	99.64	I4B-Pb1B-I3B^{ii}	87.49	86.68	81.07

I1A^{i}-Pb1A-I3A^{ii}	94.88	92.85	76.20	I1B^{i}-Pb1B-I3B^{ii}	82.69	82.13	76.16
δ2	39.57974	39.38624	66.43555	δ2	45.03340	72.89371	71.43020
	i = 1-*x*, ½+*y*, -*z*; *ii*= -1+ *x*, *y*, *z*						

Table S7. Compressibility related to crystallographic axes calculated for the phase **V** of MHy_2PbI_4 calculated in the range between 0.22 MPa and 1.00 GPa with Birch-Murnaghan coefficients.

Axes	K(TPa^{-1})	σK(TPa^{-1})	Direction			Empirical parameters			
			a	*b*	*c*	ε_0	λ	P_c	v
X_1	36.9659	4.4405	-1.00	-0.00	0.00	-3.4584e-04	-4.0863e-02	0.0010	0.6343
X_2	10.0949	4.0684	-0.00	1.00	-0.00	8.6470e-01	-7.5689e-01	-4.3481	0.0902
X_3	6.5380	4.7743	0.00	0.00	1.00	1.6208e-03	-1.0584e-02	0.0010	1.0849
V	53.0693	2.8529							

Birch-Murnaghan Coefficients

	B_0 (GPa)	σB_0 (GPa)	V_0 (Å^3)	σV_0 (Å^3)	*B*'	σ*B*'	P_c (GPa)
2nd	16.0973	0.7856	758.5795	3.6996	4	0.9872	0

Table S8. Compressibility related to crystallographic axes calculated for the phase **VI** of MHy_2PbI_4 calculated in the range between 1.30 GPa and 3.00 GPa with Birch-Murnaghan coefficients.

Axes	K(TPa^{-1})	σK(TPa^{-1})	Direction			Empirical parameters			
			a	*b*	*c*	ε_0	λ	P_c	v
X1	21.1055	9.3120	-0.0000	-1.0000	0.0000	-7.8157e-04	-2.1715e-02	1.3000	0.9782
X2	76.5033	8.5744	-1.0000	0.0000	0.0000	3.0333e-02	-3.3787e-02	1.3000	1.7945
X3	26.4176	4.5864	0.0000	0.0000	1.0000	1.4812e-02	-9.2386e-03	1.3000	2.0828
V	35.0186	1.2362							

Birch-Murnaghan Coefficients

	B_0 (GPa)	σB_0 (GPa)	V_0 (Å^3)	σV_0 (Å^3)
2nd	19.4616	1.7843	739.0541	5.4497
3rd	25.3861	17.2840	731.2967	19.7901

Table S9. Compressibility related to crystallographic axes calculated for the phase **VII** of MHy_2PbI_4 calculated in the range between 3.74 GPa and 4.2 GPa with Birch-Murnaghan coefficients.

Axes	K(TPa^{-1})	σK(TPa^{-1})	Direction		
			a	*b*	*c*
X_1	40.9690	0.0000	0.2003	-0.0000	0.9797
X_2	-8.1643	0.0000	0.0000	1.0000	-0.0000
X_3	-11.5666	0.0000	-0.9997	0.0000	0.0255
V	21.5603	0.0000			

Birch-Murnaghan Coefficients

	B_0 (GPa)	σB_0 (GPa)	V_0 (Å^3)	σV_0 (Å^3)
2nd	31.0261	2.9876	1415.0668	0.0000

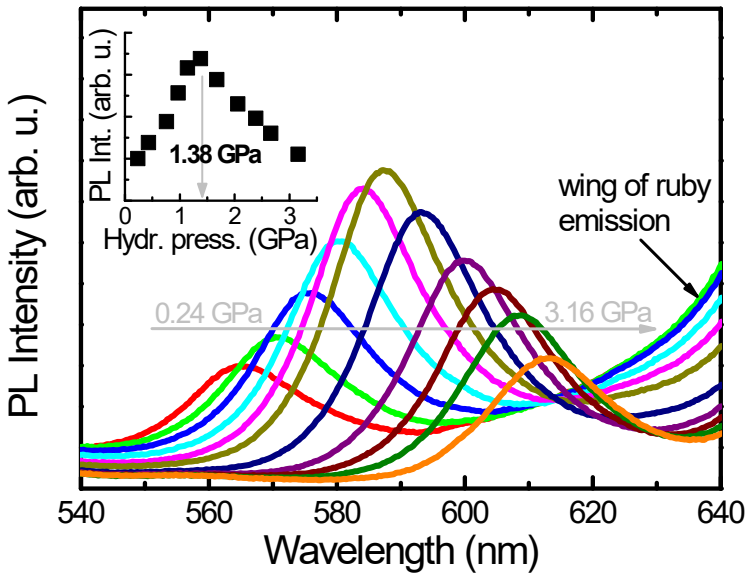

Figure S5. The emission spectra of the compressed MHy_2PbI_4 crystals with the extracted intensity of PL peak (inset).

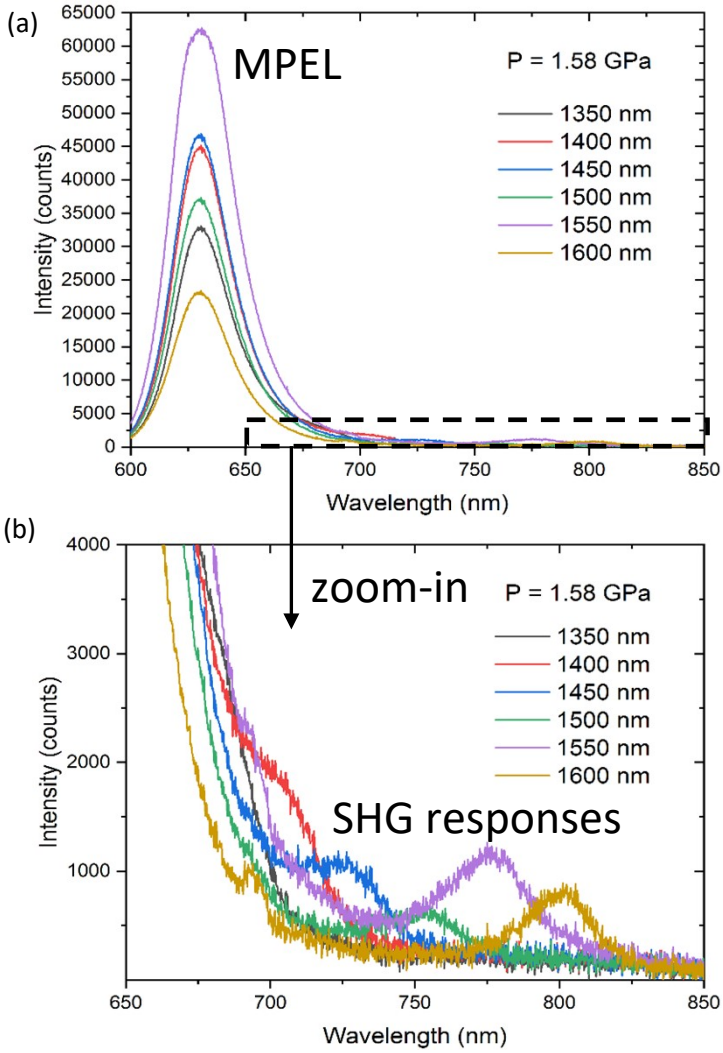

Figure S6. Nonlinear optical emissions obtained upon irradiation of MHy_2PbI_4 at 1.58 GPa with femtosecond laser pulses at different wavelengths (1350 – 1600 nm with 50 nm step). MPEL signals do not shift with wavelength change (a) while SHG signals are found at λ/2 each, see zoomed-in panel (b).

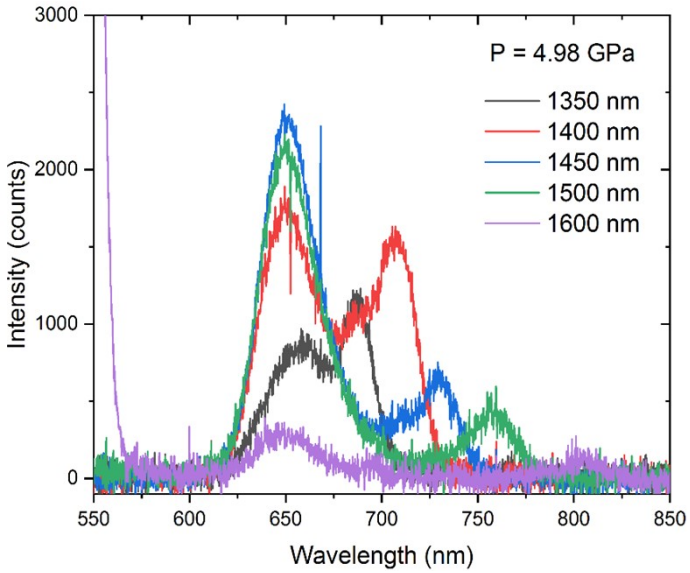

Figure S7. Nonlinear optical emissions obtained upon irradiation of MHy_2PbI_4 at 4.98GPa with femtosecond laser pulses at different wavelengths (1350 – 1600 nm with 50 nm step). MPEL signals do not shift with wavelength change while SHG signals are found at λ/2.

Table S10. Wavenumber intercepts at zero pressure (ω_0) and pressure coefficients (ω=dα/dP), obtained from fitting of the experimental data by linear functions, for the phases V, VI and VII of MHy_2PbI_4.

phase **V** 0.07 – 1.15 GPa		phase **V** 1.15 – 3.10		Phase **IV** **3.10-4.2**		Assignment
ω_0 (cm^{-1})	α	ω_0 (cm^{-1})		ω_0 (cm^{-1})		
				2987.5	-6.7	$\nu_s(CH_3)$
2954	2.9	2963.3	1.3	2965.6	2.3	$\nu_s(CH_3)$
2673.1	0.5	2672.9	0.2	2673.7	-2.7	overtone
2465.6	0.8	2467	1.3	2467.9	7.0	overtone
1606.8	-1.1	1594.5	-1.3	1592.7	-9.0	$\delta(NH_2)$
1570.5	-4.0	1553.0	-3.8	1549.0	-19.0	$\delta(NH_2^+)$
				1536.5	-76.7	$\delta(NH_2^+)$
1445.25	-1.1	1442.2	-0.8	1443.4	-2.0	$\delta_{as}(CH_3)$
				1431.9	-3.3	$\delta_{as}(CH_3)$
1408.95	-1.5	1405.2	-3.8	1404.4	-1.7	$\delta_s(CH_3)$
				1211.1	5.0	$\rho(CH_3)+\omega(NH_2)$
1200.0	-0.3	1193.3	6.2	1192.5	-3.3	$\rho(CH_3)+\omega(NH_2)$
1134.0	-0.3	1137.5	-1.5	1137.7	-5.0	$\tau(NH_2^+)+\rho(CH_3)$
1090.3	1.4	1097.6	0.2	1098.5	4.7	$\rho(CH_3)+\tau(NH_2^+)$
				1020.6	3.3	$\nu_{as}(CNN)$
976.95	0.1	989	-0.3	993.25	14.0	$\nu_{as}(CNN)$
877.66	5.0	891.7	3.0	894.7	13.0	$\nu_s(CNN)$
				862.8	10.0	$\nu_s(CNN)$
850.24	-5.4	836.7	-1.5	836.9	-0.7	$\rho(NH_2^+)$
				481.9	-41.7	δ(CNN)
434.5	4.3	450.6	-0.3	452.3	7.0	δ(CNN)
		352.6	8.3	354.5	17.3	$\tau(NH_2)$
		314.9	-0.2	310.8	-7.7	$\tau(NH_2)$
209.3	16.9	259.1	1.2	262.1	17.3	$L(MHy^+)$+ $T'(MHy^+)$+ Pb-I stretch
165.6	0.6	182.9	6.3	188.5	23.7	$L(MHy^+)$+ $T'(MHy^+)$+ Pb-I stretch

* assignment is adopted from Maczka, M.; Ptak, M. *J. Phys.Chem. C* **2022**, *126*, 7991-7998. ν_s, ν_{as}, δ, ρ, ω and τ denote symmetric stretching, antisymmetric stretching, scissoring, rocking, wagging and twisting vibrations. L and T' correspond to the librational andtranslational modes, respectively.

Table S11. Detailed crystallographic data for MHy_2PbI_4 at high-pressure.

Pressure		**0.22 GPa**	**1.00 GPa**	**1.30 GPa**	**1.70 GPa**	**2.10 GPa**	**2.64 GPa**
CCDC numbers		2298911	2298912	2298913	2298914	2298915	2298916
Crystal system		orthorhombic	orthorhombic	orthorhombic	orthorhombic	orthorhombic	orthorhombic
Space group		*Pmmn*	*Pmmn*	$Pmn2_1$	$Pmn2_1$	$Pmn2_1$	$Pmn2_1$
Unit cell dimensions	*a* (Å)	18.4404(15)	17.9087(11)	17.8170(11)	17.6111(2)	17.571(18)	17.24(3)
	b (Å)	6.35(9)	6.30(5)	6.2811(10)	6.2619(2)	6.1827(2)	6.1573(5)
	c (Å)	6.3926(14)	6.3600(8)	6.22(6)	6.201(9)	6.2444(2)	6.2293(4)
Unit cell angles	*α* (°)	90	90	90	90	90	90
	β (°)	90	90	90	90	90	90
	γ (°)	90	90	90	90	90	90
Volume ($Å^3$)		748(10)	718(6)	696(7)	683.8(10)	678.4(7)	661.3(12)
Z/*Z'*		2/0.5	2/0.5	2/0.5	2/0.5	2/0.5	2/0.5
Molecular volume (V/*Z*)		374	359	348	341.9	339.2	330.65
Calculated density (g/cm^3)		3.650	3.808	3.860	3.929	3.960	4.063
Absorption (mm^{-1})		19.482	20.312	20.957	21.331	21.501	22.057
F(000)		696	668	696	696	696	696
Crystal size (mm)		0.175 × 0.131 × 0.03	0.175 × 0.131 × 0.03	0.173 × 0.131 × 0.03	0.175 × 0.131 × 0.03	0.175 × 0.131 × 0.03	0.175 × 0.131 × 0.03
2θ-range for data collection (°)		6.746 to 52.49	6.798 to 52.57	6.878 to 53.60	6.506 to 54.828	6.59 to 55.296	9.31 to 52.296
Min/max indices: *h*, *k*, *l*		-5 ≤ h ≤ 5, -6 ≤ k ≤ 7, -7 ≤ l ≤ 7	-5 ≤ h ≤ 5, -6 ≤ k ≤ 7, -7 ≤ l ≤ 7	-5 ≤ h ≤ 5, -7 ≤ k ≤ 7, -6 ≤ l ≤ 7	-5 ≤ h ≤ 5, -8 ≤ k ≤ 8, -8 ≤ l ≤ 7	-4 ≤ h ≤ 4, -8 ≤ k ≤ 7, -8 ≤ l ≤ 7	-4 ≤ h ≤ 4, -7 ≤ k ≤ 7, -7 ≤ l ≤ 7
Reflect. Collected/unique		1351/236	2141/252	1298/363	3891/511	3249/434	2880/354
Data/restrains/parameters		236/90/41	252/45/41	363/70/57	511/46/56	434/45/57	354/71/56
Goodness-of-fit on F^2		1.149	1.192	1.011	1.154	1.132	1.124
Final R1/wR2 (I>2σ1)		0.0844/0.2146	0.0425/0.0947	0.0720/0.1613	0.0276/0.0674	0.0244/0.0484	0.0491/0.1084
R_1/wR_2 (all data)		0.0936/0.2270	0.0511/0.0964	0.0873/0.1734	0.0273/0.0678	0.0251/0.0490	0.0528/0.1124
Largest diff. peak/hole ($e.Å^{-3}$)		1.28/-1.07	0.87/-0.69	1.36/-1.01	0.82/-0.77	0.71/-0.60	1.22/-1.28

$w=1/(\sigma^2F_o^2+w_1^2*P^2+w_2*P)$, where $P=(Max(F_o^2,0)+2*Fc^2)$

Table S12. Detailed crystallographic data for MHy_2PbI_4 at high-pressure.

Pressure		**3.00 GPa**	**3.30 GPa**	**3.74 GPa**	**4.20 GPa**
CCDC numbers		2298917	2298918	2298919	2298920
Crystal system		orthorhombic	monoclinic	monoclinic	monoclinic
Space group		$Pmn2_1$	$P2_1$	$P2_1$	$P2_1$
Unit cell dimensions	*a* (Å)	17.19(2)	6.1212(3)	6.0985(2)	6.1302(5)
	b (Å)	6.2150(3)	12.3727(7)	12.3284(4)	12.3747(10)
	c (Å)	6.1341(3)	17.150(5)	17.049(5)	16.73(3)
Unit cell angles	*α* (°)	90	90	90	90
	β (°)	90	90.095(13)	90.097(12)	90.30(3)
	γ (°)	90	90	90	90
Volume ($Å^3$)		655.3(8)	1298.9(4)	1281.8(4)	1269(2)
Z/*Z*'		2/0.5	4/2	4/2	4/2
Molecular volume (V/*Z*)		327.65	324.725	320.45	317.25
Calculated density (g/cm^3)		4.100	4.137	4.192	4.234
Absorption (mm^{-1})		22.259	22.459	22.759	22.988
F(000)		696	1392	1392	1392
Crystal size (mm)		0.19 x 0.16 x 0.05	0.17 x 0.13 x 0.03	0.17 x 0.13 x 0.03	0.21 x 0.13 x 0.015
2θ-range for data collection (°)		9.338 to 52.31	6.586 to 52.628	6.61 to 53.206	6.586 to 52.706
Min/max indices: *h*, *k*, *l*		-3 ≤ h ≤ 3, -7 ≤ k ≤ 7, -7 ≤ l ≤ 7	-7 ≤ h ≤ 7, -15 ≤ k ≤ 15, -4 ≤ l ≤ 4	-7 ≤ h ≤ 7, -15 ≤ k ≤ 15, -3 ≤ l ≤ 3	-7 ≤ h ≤ 7, -15 ≤ k ≤ 15, -5 ≤ l ≤ 4
Reflect. Collected/unique		2388/309	5966/974	6025/926	6862/1331
Data/restrains/parameters		309/85/56	974/9/43	926/1/43	1331/1/47
Goodness-of-fit on F^2		1.186	1.115	1.041	1.101
Final R1/wR2 (I>2σ1)		0.0435/0.0829	0.1556/0.2915	0.1645/0.3629	0.1730/0.3591
R_1/wR_2 (all data)		0.0469/0.0862	0.1887/0.3139	0.1789/0.3752	0.1849/0.3691
Largest diff. peak/hole ($e.Å^{-3}$)		0.91/-0.97	2.37/-2.72	2.89/-3.95	3.92/-4.04

$w=1/(\sigma^2F_o^2+w_1^2*P^2+w_2*P)$, where $P=(Max(F_o^2,0)+2*Fc^2)$

Table S13. Detailed crystallographic data for MHy_2PbI_4 at high-temperature.

Temperature		**300 K**	**310 K**	**320 K**	**330 K**	**340 K**	**360 K**	**370 K**
CCDC numbers		2298904	2298905	2298906	2298907	2298908	2298909	2298910
Crystal system		orthorhombic	orthorhombic	orthorhombic	orthorhombic	orthorhombic	orthorhombic	orthorhombic
Space group		*Pmcn*	*Pmcn*	*Pmmn*	*Pmmn*	*Pmmn*	*Pmmn*	*Pmmn*
Unit cell dimensions	*a* (Å)	18.684(4)	18.7116(5)	18.7487(6)	18.7824(6)	18.8229(6)	18.9231(9)	18.9775(10)
	b (Å)	6.3720(13)	6.3719(2)	6.3729(2)	6.3740(2)	6.3753(2)	6.3804(2)	6.3842(2)
	c (Å)	12.769(3)	12.7687(3)	6.3843(2)	6.3845(2)	6.3839(2)	6.3828(2)	6.3817(3)
Unit cell angles	*α* (°)	90	90	90	90	90	90	90
	β (°)	90	90	90	90	90	90	90
	γ (°)	90	90	90	90	90	90	90
Volume (Å^3)		1520.2(5)	1522.39(7)	762.82(4)	764.35(4)	766.08(4)	770.64(5)	773.18(6)
Z/*Z*'		4/0.5	4/0.5	2/0.25	2/0.25	2/0.25	2/0.25	2/0.25
Molecular volume (V/*Z*)		380.05	380.59	381.41	382.175	383.04	385.32	386.59
Calculated density (g/cm^3)		3.535	3.530	3.522	3.514	3.446	3.425	3.414
Absorption (mm^{-1})		19.190	19.162	19.121	19.086	19.038	18.925	18.863
F(000)		1392	1392	696	682	668	668	668
Crystal size (mm)		0.15 x 0.10 x 0.08	0.15 x 0.10 x 0.08	0.15 x 0.10 x 0.08	0.15 x 0.10 x 0.08	0.15 x 0.10 x 0.08	0.15 x 0.10 x 0.08	0.15 x 0.10 x 0.08
2θ-range for data collection (°)		6.382 to 58.168	6.382 to 58.168	6.382 to 57.694	6.382 to 57.948	6.382 to 57.874	6.384 to 57.734	6.384 to 58.27
Min/max indices: *h*, *k*, *l*		-25 ≤ h ≤ 24, -8 ≤ k ≤ 8, -16 ≤ l ≤ 17	-24 ≤ h ≤ 25, -8 ≤ k ≤ 8, -16 ≤ l ≤ 17	-24 ≤ h ≤ 25, -8 ≤ k ≤ 8, -8 ≤ l ≤ 8	-24 ≤ h ≤ 25, -8 ≤ k ≤ 8, -8 ≤ l ≤ 8	-24 ≤ h ≤ 25, -8 ≤ k ≤ 8, -8 ≤ l ≤ 8	-24 ≤ h ≤ 25, -8 ≤ k ≤ 8, -8 ≤ l ≤ 8	-26 ≤ h ≤ 24, -8 ≤ k ≤ 8, -8 ≤ l ≤ 8
Reflect. Collected/unique		13638/1943	13671/1945	7002/1058	7079/1061	7032/1057	7005/1056	6997/1050
Data/restrains/parameters		1943/24/57	1945/36/57	1058/41/47	1061/44/46	1057/3/49	1056/50/46	1050/46/49
Goodness-of-fit on F^2		1.005	0.985	1.105	1.116	1.188	1.087	1.134
Final R1/wR2 (I>2σ1)		0.0396/0.0806	0.0403/0.0827	0.0384/0.0845	0.0444/0.1035	0.0458/0.1057	0.0613/0.1523	0.0741/0.1795
R_1/wR_2 (all data)		0.0855/0.0976	0.0874/0.1005	0.0478/0.0883	0.0537/0.1080	0.0567/0.1106	0.0745/0.1613	0.0984/0.1946
Largest diff. peak/hole (e.Å^{-3})		1.93/-1.36	1.87/-1.17	2.07/-1.09	1.80/-1.07	1.75/-1.08	4.17/-1.21	5.04/-1.68

$w=1/(\sigma^2F_o^2+w_1^2*P^2+w_2*P)$, where $P=(Max(F_o^2,0)+2*Fc^2)$